Arch. Mech., **62**, 3, pp. 177–193, Warszawa 2010

Thermoelastic waves at an interface between two solid half-spaces under hydrostatic initial stress

B. SINGH[1], J. SINGH[2], P. AILAWALIA[3]

[1] *Department of Mathematics*
Government College
Sector-11, Chandigarh-160011, India
e-mail: bsinghgc11@gmail.com

[2] *Department of Mathematics*
Indo Global College of Engineering
Abhipur, Mohali, India

[3] *Department of Mathematics*
RIMT Institute of Engineering and Technology
Mandi Govindgarh, Punjab, India

A model of two semi-infinite half-spaces of different thermoelastic solids is considered in welded contact under hydrostatic initial stress. The appropriate boundary conditions are satisfied at the interface to obtain the reflection and refraction coefficients of various reflected and refracted waves during incidence of the quasi-thermal wave. A particular numerical example is considered to show the effect of hydrostatic initial stress on these coefficients for a certain range of the angle of incidence.

Key words: thermoelasticity, hydrostatic initial stress, reflection, refraction, relaxation time.

Notations

u_i $(i = 1, 2)$	components of displacement vectors,
T_0	uniform absolute temperature,
T	temperature above the reference temperature,
ρ_0	mass density,
C_e	specific heat at constant strain,
τ_0	thermal relaxation time,
K	thermal conductivity,
α	coefficient of linear thermal expansion,
p	initial pressure,
$\overline{\lambda}, \overline{\mu}$	counterparts of Lamé parameters,
φ, ψ	potential functions,
k	wave number,
c	wave speed,

$\omega = kc$ frequency,
$\Theta = T - T_0$ change in temperature,
q_i heat flux vector,
$K_T = (3\overline{\lambda} + 2\overline{\mu})^{-1}$
All quantities with primes correspond to medium M'.

1. Introduction

The classical theory of thermoelasticity, the foundations of which were laid in the nineteenth century by Duhamel, Neumann and Lord Kelvin, is based on Fourier's law of heat conduction [1]. When combined with other laws of mechanics and thermodynamics, such as the geometrical relations, equations of motion, conservation of energy law, dissipation inequality and constitutive relations, Fourier's law gives rise to the displacement-temperature field equations of hyperbolic-parabolic type that imply an infinite speed of propagation of thermoelastic waves. To correct this unrealistic feature, various modifications of the classical theory of thermoelasticity have been proposed. For example, Lord and Shulman [2] developed the theory of generalized thermoelasticity with one relaxation time for the special case of an isotropic body. Green and Lindsay [3] developed the theory of thermoelasticity after taking two relaxation times. The above two theories allow a finite speed of propagation of waves. Chandrasekharaiah [4] referred to this wavelike thermal disturbance as a "second sound". The representative theories in the range of generalized thermoelasticity were reviewed by Hetnarski and Ignaczak [5].

The wave propagation in thermoelastic media is applicable in various fields such as earthquake engineering, soil dynamics, nuclear reactors, high energy particle accelerators, etc. Many authors have studied the wave propagation in isotropic thermoelasticity. For example, Deresiewicz [6] studied the effects of boundaries on the waves in a thermoelastic solid and reflection of plane waves from a plane boundary. Sinha and Sinha [7] and Sinha and Elsibai [8] discussed the reflection of thermoelastic waves at a solid half-space in context of the Lord and Shulman [2] and Green and Lindsay [3] theories. Abd-Alla [9] studied the relaxation effects on reflection of generalized magneto-thermoelastic waves. Singh [10] discussed the reflection of a plane sound wave from a micropolar generalized thermoelastic solid half-space. Sharma *et al.* [11] studied the problem of Sinha and Sinha [7] for various linear theories of thermoelasticity. Sinha and Elsibai [12] studied the reflection of thermoelastic waves at the interface of two semi-infinite media being in welded contact. Singh [13] and Abd-Alla *et al.* [14] discussed some problems concerning reflection of the generalized magneto-thermo-viscoelastic plane waves from a stress-free surface. Singh [15] discussed the reflection of SV waves from the free surface of an elastic solid with generalized thermoelastic diffusion. Song *et. al.* [16] studied the wave propagation at interface between two half-spaces of micropolar viscoelastic media. Singh [17] studied the reflection of waves from free surface of the generalized thermoelastic solid with voids. Kumar and Singh [18] discussed the reflection and transmission at an imperfectly bounded interface between two orthotropic, generalized thermoelastic half-spaces. Othman and Song [19] discussed the reflection of magneto-thermoelastic waves with two relaxation times and temperature-dependent elastic moduli. The study of wave propagation in an isotropic generalized thermoelastic solid with additional parameters provide information about the existence of new or modified waves. Such information may be useful for experimental seismologists in correcting the earthquake estimation.

The development of initial stresses in the medium is due to many reasons, for example resulting from the difference of temperature, process of quenching, shot peening and cold working, slow process of creep, differential external forces, gravity variations etc. The Earth is assumed to be under high initial stresses. It is therefore of much interest to study the influence of these stresses on the propagation of stress waves. Biot [20] showed the acoustic propagation under initial stresses which was fundamentally different from that under stress-free state. He has obtained the velocities of longitudinal and transversal waves along the co-ordinate axis only. The study of reflection and refraction phenomena of plane waves in unbounded medium under initial stresses is due to Chattopadhyay *et al.* [21], Sidhu and Singh [22], Dey *et al.* [23] and Selim [24].

Montanaro [25] investigated the isotropic linear thermoelasticity with hydrostatic initial stress. Singh *et al.* [26], Singh [27] and Othman and Song [28] used the theory given by Montanaro [25] and studied the reflection of thermoelastic waves from a free surface under hydrostatic initial stress, in context of different theories of the generalized thermoelasticity. The problems concerning reflection and refraction of elastic waves at a plane separating two media have wide applications in seismic-reflection surveys. In the present paper, the Montanaro [25] theory of thermoelasticity with hydrostatic initial stresses is employed to study an interface model between two thermoelastic media under hydrostatic initial stresses. The boundary conditions at the interface are formulated and are satisfied by appropriate potentials to obtain the expression of reflection and refraction coefficients, both theoretically as well as numerically. The reflection and refraction coefficients are computed for a particular model and the numerical results are shown graphically to show the effect of initial stresses on the reflection and refraction coefficients of various reflected and refracted waves.

2. Governing equations and solution

The field equations in the x-y plane for homogeneous, isotropic thermoelastic solid with hydrostatic initial stress and in absence of incremental body forces and heat sources, are [2, 25]:

$$\overline{V}_T^2 \frac{\partial^2 u_1}{\partial x^2} + (\overline{V}_T^2 - \overline{V}_S^2)\frac{\partial^2 u_2}{\partial x\, \partial y} + \overline{V}_S^2 \frac{\partial^2 u_1}{\partial y^2} - \beta \frac{\partial \Theta}{\partial x} = \frac{\partial^2 u_1}{\partial t^2}, \tag{2.1}$$

$$\overline{V}_T^2 \frac{\partial^2 u_2}{\partial y^2} + (\overline{V}_T^2 - \overline{V}_S^2)\frac{\partial^2 u_1}{\partial x\, \partial y} + \overline{V}_S^2 \frac{\partial^2 u_2}{\partial x^2} - \beta \frac{\partial \Theta}{\partial y} = \frac{\partial^2 u_2}{\partial t^2}, \tag{2.2}$$

$$\begin{aligned}\frac{K}{\rho_0}\left(\frac{\partial^2 \Theta}{\partial x^2} + \frac{\partial^2 \Theta}{\partial y^2}\right) \\ = C_e\left(1 + \tau_0 \frac{\partial}{\partial t}\right)\frac{\partial \Theta}{\partial t} + \beta T_0 \left(1 + \tau_0 \frac{\partial}{\partial t}\right)\frac{\partial}{\partial t}\left(\frac{\partial u_1}{\partial x} + \frac{\partial u_2}{\partial y}\right),\end{aligned} \tag{2.3}$$

where

$$\overline{V}_T = \sqrt{\frac{\overline{\lambda} + 2\overline{\mu}}{\rho_0}}, \qquad \overline{V}_S = \sqrt{\frac{\overline{\mu} - p/2}{\rho_0}}, \qquad \beta = \frac{\alpha}{K_T \rho_0} \tag{2.4}$$

and the symbols have their usual meanings.

Using the displacement components u_1 and u_2 in terms of potential functions φ and ψ as

$$u_1 = \frac{\partial \varphi}{\partial x} - \frac{\partial \psi}{\partial y}, \qquad u_2 = \frac{\partial \varphi}{\partial y} + \frac{\partial \psi}{\partial x}, \tag{2.5}$$

the Eqs. (2.1)–(2.3) are transformed to

$$\overline{V}_T^2 \nabla^2 \varphi - \beta \Theta = \frac{\partial^2 \varphi}{\partial t^2}, \tag{2.6}$$

$$\overline{V}_S^2 \nabla^2 \psi = \frac{\partial^2 \psi}{\partial t^2}, \tag{2.7}$$

$$\frac{K}{\rho_0}\nabla^2 \Theta = C_e\left(1 + \tau_0 \frac{\partial}{\partial t}\right)\frac{\partial \Theta}{\partial t} + \beta T_0 \left(1 + \tau_0 \frac{\partial}{\partial t}\right)\frac{\partial}{\partial t}\nabla^2 \varphi. \tag{2.8}$$

Equations (2.6) and (2.8) are coupled in φ and Θ, whereas Eq. (2.7) is uncoupled.

Solutions of Eqs. (2.6) and (2.8) are now sought in the form of a harmonic travelling wave

$$(\varphi, \Theta) = (A, B) e^{ik(x \sin\theta + y \cos\theta - ct)}, \tag{2.9}$$

where $(\sin\theta, \cos\theta)$ denotes the projection of the wave normal onto the x-y plane and A, B are arbitrary constants.

Using (2.9) in Eqs. (2.6) and (2.8), the following quadratic equation in c^2 is obtained:

$$L(c^2)^2 - Mc^2 + N = 0, \tag{2.10}$$

where

$$\begin{aligned} L &= C_e\tau^*, \qquad M = \frac{K}{\rho_0} + \overline{V}_T^2\tau^* C_e + \beta^2 T_0\tau^*, \\ N &= \frac{\overline{V}_T^2 K}{\rho_0}, \qquad \tau^* = \tau_0 + \left(\frac{i}{\omega}\right). \end{aligned} \tag{2.11}$$

The roots

$$c_1^2 = \frac{M + \sqrt{M^2 - 4LN}}{2L}, \qquad c_2^2 = \frac{M - \sqrt{M^2 - 4LN}}{2L} \tag{2.12}$$

of Eq. (2.10) correspond to the complex speeds of quasi-P (qP) wave and quasi-thermal (qT) wave, respectively. If we write $c_j^{-1} = v_j^{-1} - i\omega^{-1}q_j^*$ $(j = 1, 2)$, then v_1 and v_2 are the speeds of propagation of a quasi-P wave and quasi-thermal wave, respectively. q_1^* and q_2^* are attenuations of qP and qT waves, respectively. Also, the solution of Eq. (2.7) gives the wave speed of a shear wave as $v_3 = \overline{v}_s$.

3. Reflection and refraction

Two semi-infinite half-spaces of thermoelastic media under hydrostatic initial stresses are assumed to be in welded contact with interface along the x-axis and the direction of positive y-axis is directed into the lower medium M. For the incidence of qT wave passing through medium M, at interface $y = 0$, the qP, qT and SV waves will be reflected in lower medium M and qP, qT and SV waves will be refracted in upper medium M'. The complete geometry showing the angle of incidence, angles of reflection and angles of refraction are shown in Fig. 1. The required boundary conditions at the interface $y = 0$ are the continuity of normal stress, tangential stress, heat flux, temperature, tangential and normal components of displacement vector, i.e.

$$\sigma_{yy} = \sigma'_{yy}, \quad \sigma_{yx} = \sigma'_{yx}, \quad q_y = q'_y, \quad \Theta = \Theta', \quad u_1 = u'_1, \quad u_2 = u'_2 \tag{3.1}$$

where

$$\begin{aligned} \sigma_{yy} &= -p + \overline{\lambda}\frac{\partial^2\varphi}{\partial x^2} + (\overline{\lambda} + 2\overline{\mu})\frac{\partial^2\varphi}{\partial y^2} + 2\overline{\mu}\frac{\partial^2\Psi}{\partial x\partial y} - \frac{\alpha}{K_T}\Theta, \\ \sigma_{yx} &= \frac{p}{2}\nabla^2\Psi + \overline{\mu}\left(2\frac{\partial^2\varphi}{\partial x\partial y} + \frac{\partial^2\Psi}{\partial x^2} - \frac{\partial^2\Psi}{\partial y^2}\right), \\ \sigma'_{yy} &= -p + \overline{\lambda}'\frac{\partial^2\varphi'}{\partial x^2} + (\overline{\lambda}' + 2\overline{\mu}')\frac{\partial^2\varphi'}{\partial y^2} + 2\overline{\mu}'\frac{\partial^2\Psi'}{\partial x\partial y} - \frac{\alpha'}{K'_T}\Theta', \end{aligned}$$

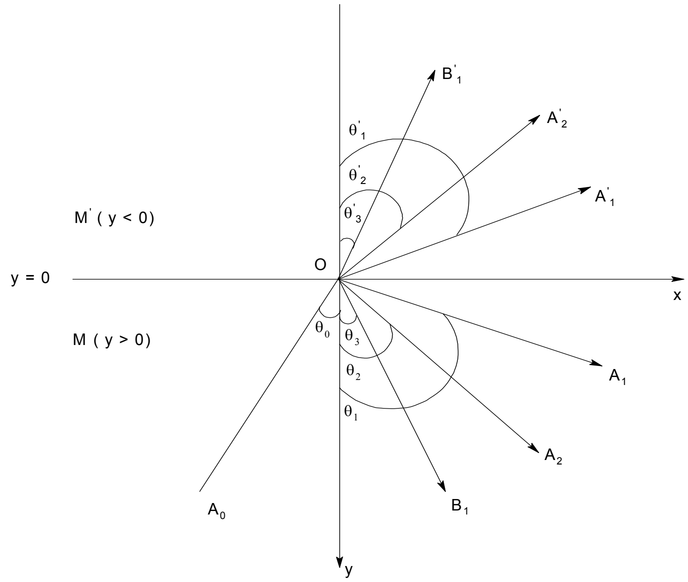

FIG. 1. Schematic diagram for the problem.

$$\sigma'_{yx} = \frac{p}{2}\nabla^2\Psi' + \overline{\mu}'\left(2\frac{\partial^2\varphi'}{\partial x\partial y} + \frac{\partial^2\Psi'}{\partial x^2} - \frac{\partial^2\Psi'}{\partial y^2}\right),$$

$$q_y = -\frac{K}{1+\tau_0\dfrac{\partial}{\partial t}}\frac{\partial\Theta}{\partial y}, \qquad q'_y = -\frac{K'}{1+\tau'_0\dfrac{\partial}{\partial t}}\frac{\partial\Theta'}{\partial y},$$

$$u'_1 = \frac{\partial\varphi'}{\partial x} - \frac{\partial\Psi'}{\partial y}, \qquad u'_2 = \frac{\partial\varphi'}{\partial y} + \frac{\partial\Psi'}{\partial x}.$$

The appropriate potentials satisfying the boundary conditions (3.1) are as follows:

For medium M:

$$\begin{aligned}\varphi = A_0 \exp[ik_2(x\sin\theta_0 + y\cos\theta_0) - i\omega t] \\ + A_1 \exp[ik_1(x\sin\theta_1 - y\cos\theta_1) - i\omega t] \\ + A_2 \exp[ik_2(x\sin\theta_2 - y\cos\theta_2) - i\omega t],\end{aligned} \tag{3.2}$$

$$\begin{aligned}\Theta = \varepsilon_2 A_0 \exp[ik_2(x\sin\theta_0 + y\cos\theta_0) - i\omega t] \\ + \varepsilon_1 A_1 \exp[ik_1(x\sin\theta_1 - y\cos\theta_1) - i\omega t] \\ + \varepsilon_2 A_2 \exp[ik_2(x\sin\theta_2 - y\cos\theta_2) - i\omega t],\end{aligned} \tag{3.3}$$

$$\Psi = B_1 \exp[ik_3(x\sin\theta_3 - y\cos\theta_3) - i\omega t], \tag{3.4}$$

where

$$\varepsilon_i = \frac{k_i^2(v_i^2 - \overline{v}_T^2)}{\beta}, \qquad i = 1, 2, 3,$$

and A_0, A_1, A_2 and B_1 are amplitudes of incident qT wave, reflected qP wave, reflected qT wave and reflected SV wave, respectively.

For medium M':

$$\varphi' = A_1' \exp[ik_1'(x \sin\theta_1' + y\cos\theta_1') - i\omega t] + A_2' \exp[ik_2'(x \sin\theta_2' + y\cos\theta_2') - i\omega t], \tag{3.5}$$

$$\Theta' = \varepsilon_1' A_1' \exp[ik_1'(x \sin\theta_1' + y\cos\theta_1') - i\omega t] + \varepsilon_2' A_2' \exp[ik_2'(x \sin\theta_2' + y\cos\theta_2') - i\omega t], \tag{3.6}$$

$$\Psi' = B_1' \exp[ik_3'(x \sin\theta_3' + y\cos\theta_3') - i\omega t], \tag{3.7}$$

where

$$\varepsilon_i' = \frac{k_i'(v_i'^2 - \overline{v}_T'^2)}{\beta'}, \qquad i = 1, 2, 3,$$

and A_1', A_2' and B_1' are amplitudes of the refracted qP wave, refracted qT wave and refracted SV wave, respectively.

These potentials will satisfy the boundary conditions (3.1) at $y = 0$, if k_j, k_j', θ_j, θ_j' $(j = 1, 2, 3)$ are related as:

$$k_2 \sin\theta_0 = k_1 \sin\theta_1 = k_2 \sin\theta_2 = k_3 \sin\theta_3 = k_1' \sin\theta_1' = k_2' \sin\theta_2' = k_3' \sin\theta_3', \tag{3.8}$$

i.e.

$$\frac{\sin\theta_0}{v_2} = \frac{\sin\theta_1}{v_1} = \frac{\sin\theta_2}{v_2} = \frac{\sin\theta_3}{v_3} = \frac{\sin\theta_1'}{v_1'} = \frac{\sin\theta_2'}{v_2'} = \frac{\sin\theta_3'}{v_3'}. \tag{3.9}$$

Using the potential given by Eqs. (3.2) to (3.7) in Eq. (3.1), a system of six non-homogeneous equations is obtained as

$$\sum_{i=1}^{6} a_{ij} Z_j = b_i, \qquad i = 1, 2, \ldots, 6, \tag{3.10}$$

where a_{ij} are as follows:

$$a_{11} = -\left(\frac{v_2}{v_1}\right)^2 \left[\frac{\overline{\lambda}}{\overline{\mu}} + 2\left(1 - \left(\frac{v_1}{v_2}\right)^2 \sin^2\theta_0\right) + \frac{v_1^2 - \overline{v}_T^2}{(\overline{\mu}/\rho_0)}\right],$$

$$a_{12} = -\left(\frac{\overline{\lambda}}{\overline{\mu}} + 2\cos^2\theta_0\right) - \frac{v_2^2 - \overline{v}_T^2}{(\overline{\mu}/\rho_0)},$$

$$a_{13} = 2\left(\frac{v_2}{v_3}\right)\sin\theta_0\sqrt{1-\left(\frac{v_3}{v_2}\right)^2\sin^2\theta_0},$$

$$a_{14} = \left(\frac{v_2}{v_1'}\right)^2\left[\frac{\overline{\lambda}'}{\overline{\mu}} + 2\frac{\overline{\mu}'}{\overline{\mu}}\left(1-\left(\frac{v_1'}{v_2}\right)^2\sin^2\theta_0\right) + \frac{v_1'^2-\overline{v}_T'^2}{(\overline{\mu}/\rho_0')}\right],$$

$$a_{15} = \left(\frac{v_2}{v_2'}\right)^2\left[\frac{\overline{\lambda}'}{\overline{\mu}} + 2\frac{\overline{\mu}'}{\overline{\mu}}\left(1-\left(\frac{v_2'}{v_2}\right)^2\sin^2\theta_0\right) + \frac{v_2'^2-\overline{v}_T'^2}{(\overline{\mu}/\rho_0')}\right],$$

$$a_{16} = 2\frac{\overline{\mu}'}{\overline{\mu}}\frac{v_2}{v_3'}\sin\theta_0\sqrt{1-\left(\frac{v_3'}{v_2}\right)^2\sin^2\theta_0},$$

$$a_{21} = 2\frac{v_2}{v_1}\sin\theta_0\sqrt{1-\left(\frac{v_1}{v_2}\right)^2\sin^2\theta_0},$$

$$a_{22} = \sin^2\theta_0,$$

$$a_{23} = \left[-\frac{p}{2\overline{\mu}} + \left(1-2\left(\frac{v_3}{v_2}\right)^2\sin^2\theta_0\right)\right]\left(\frac{v_2}{v_3}\right)^2,$$

$$a_{24} = 2\frac{\overline{\mu}'}{\overline{\mu}}\frac{v_2}{v_1'}\sin\theta_0\sqrt{1-\left(\frac{v_1'}{v_2}\right)^2\sin^2\theta_0},$$

$$a_{25} = 2\frac{\overline{\mu}'}{\overline{\mu}}\frac{v_2}{v_2'}\sin\theta_0\sqrt{1-\left(\frac{v_2'}{v_2}\right)^2\sin^2\theta_0},$$

$$a_{26} = \left[\frac{p}{2\overline{\mu}} - \frac{\overline{\mu}'}{\overline{\mu}}\left(1-2\left(\frac{v_3'}{v_2}\right)^2\sin^2\theta_0\right)\right]\left(\frac{v_2}{v_3'}\right)^2,$$

$$a_{31} = \left(\frac{v_2}{v_1}\right)^3\sqrt{1-\left(\frac{v_1}{v_2}\right)^2\sin^2\theta_0}\left(\frac{v_1^2-\overline{v}_T^2}{\beta}\right),$$

$$a_{32} = \cos\theta_0\left(\frac{v_2^2-\overline{v}_T^2}{\beta}\right),$$

$$a_{33} = 0,$$

$$a_{34} = \chi\left(\frac{v_2}{v_1'}\right)^3\sqrt{1-\left(\frac{v_1'}{v_2}\right)^2\sin^2\theta_0}\left(\frac{v_1'^2-\overline{v}_T'^2}{\beta'}\right),$$

$$a_{35} = \chi\left(\frac{v_2}{v_2'}\right)^3\sqrt{1-\left(\frac{v_2'}{v_2}\right)^2\sin^2\theta_0}\left(\frac{v_2'^2-\overline{v}_T'^2}{\beta'}\right),$$

$$a_{36} = 0,$$

$$\chi = \frac{K'}{K}\frac{1 - i\omega\tau_0}{1 - i\omega\tau_0'},$$

$$a_{41} = \left(\frac{v_2}{v_1}\right)^2 \left(\frac{v_1^2 - \overline{v}_T^2}{\beta}\right), \qquad a_{42} = \frac{v_2^2 - \overline{v}_T^2}{\beta},$$

$$a_{43} = 0, \qquad a_{44} = -\left(\frac{v_2}{v_1'}\right)^2 \left(\frac{v_1'^2 - \overline{v}_T'^2}{\beta'}\right),$$

$$a_{45} = -\left(\frac{v_2}{v_2'}\right)^2 \left(\frac{v_2'^2 - \overline{v}_T'^2}{\beta'}\right), \qquad a_{46} = 0,$$

$$a_{51} = \sin\theta_0, \qquad a_{52} = \sin\theta_0,$$

$$a_{53} = \frac{v_2}{v_3}\sqrt{1 - \left(\frac{v_3}{v_2}\right)^2 \sin^2\theta_0}, \qquad a_{54} = -\sin\theta_0,$$

$$a_{55} = -\sin\theta_0, \qquad a_{56} = \frac{v_2}{v_3'}\sqrt{1 - \left(\frac{v_3'}{v_2}\right)^2 \sin^2\theta_0},$$

$$a_{61} = \frac{v_2}{v_1}\sqrt{1 - \left(\frac{v_1}{v_2}\right)^2 \sin^2\theta_0}, \qquad a_{62} = \cos\theta_0,$$

$$a_{63} = -\sin\theta_0, \qquad a_{64} = \frac{v_2}{v_1'}\sqrt{1 - \left(\frac{v_1'}{v_2}\right)^2 \sin^2\theta_0},$$

$$a_{65} = \frac{v_2}{v_2'}\sqrt{1 - \left(\frac{v_2'}{v_2}\right)^2 \sin^2\theta_0}, \qquad a_{66} = \sin\theta_0.$$

Constants b_i and Z_j are as follows:

$$b_1 = -a_{12}, \quad b_2 = a_{22}, \quad b_3 = a_{32}, \quad b_4 = -a_{42}, \quad b_5 = -a_{52}, \quad b_6 = a_{62},$$

$$Z_1 = \frac{A_1}{A_0}, \quad Z_2 = \frac{A_2}{A_0}, \quad Z_3 = \frac{B_1}{A_0}, \quad Z_4 = \frac{A_1'}{A_0}, \quad Z_5 = \frac{A_2'}{A_0}, \quad Z_6 = \frac{B_1'}{A_0}.$$

Here, Z_1, Z_2, Z_3 are real-valued reflection coefficients (or amplitude ratios) of reflected qP, qT and SV waves respectively and Z_4, Z_5, Z_6 are real-valued refraction coefficients (or amplitude ratios) of refracted qP, qT and SV waves, respectively.

In absence of the upper medium, the system of Eqs. (3.10) reduced to those obtained by SINGH *et al.* [26].

4. Numerical results and discussion

For the purpose of numerical computations, the following physical constants are considered for medium M:

$$E = 6.9 \times 10^{11} \text{ dyne/cm}^2, \quad \sigma = 0.33, \quad \rho_0 = 2.7 \text{ g m/cm}^3,$$
$$C_e = 0.236 \text{ cal/g m}\,^\circ\text{C}, \quad K = 0.492 \text{ cal/cm s}\,^\circ\text{C}, \quad \tau_0 = 0.04 \text{ s},$$
$$\alpha = 0.01\,^\circ\text{C}^{-1}, \quad K_T = 0.5 \text{ dyne}^{-1}\text{cm}^2, \quad \omega = 2 \text{ s}^{-1}, \quad T_0 = 20\,^\circ\text{C}.$$

The relevant parameters taken for medium M' are

$$E' = 6.7 \times 10^{11} \text{ dyne/cm}^2, \quad \sigma' = 0.31, \quad \rho_0' = 2.3 \text{ gm/cm}^3,$$
$$C_e' = 0.214 \text{ cal/g m}\,^\circ\text{C}, \quad K' = 0.483 \text{ cal/cm s}\,^\circ\text{C}, \quad \tau_0' = 0.04 \text{ s},$$
$$\alpha' = 0.008\,^\circ\text{C}^{-1}, \quad K_T' = 0.45 \text{ dyne}^{-1}\text{cm}^2.$$

The relation $E/\mu = 2(1+\sigma)$for isotropic elastic solids does not hold good for earthy materials, viz. sand, soil, etc. WEISKOPF [29] investigated that due to slipping of granules on each other, the resistance of shear is much less than that in an elastic solid and the resultant shearing deflection is much greater. For these materials $E/\mu > 2(1+\sigma)$. Hence, here we define the generalized Lamé's constants $\overline{\lambda}$ and $\overline{\mu}$ as

$$\overline{\lambda} = \frac{E\sigma}{\eta(1+\sigma)(1-2\sigma)}, \qquad \overline{\mu} = \frac{E}{2\eta(1+\sigma)},$$

where E is Young's modulus, σ is Poisson's ratio and η (≥ 1) is defined as sandiness or initial stress parameter. $\eta = 1$ corresponds to isotropic elastic medium with no initial stress. Similar relations hold also in medium M'.

Using the above parameters for two different half-spaces in welded contact, the system of Eqs. (3.10) is solved with the help of FORTRAN PROGRAM of the Gauss elimination method. The absolute values of real-valued amplitude ratios (or reflection and refraction coefficients) of reflected and refracted qP, qT and SV waves, are computed numerically for the range $0^\circ < \theta_0 \leq 78^\circ$ of angle of incidence of the qT wave. The variations of these amplitude ratios are shown graphically in Figs. 2 to 7. The solid and dotted curves in these figures correspond to amplitude ratios in presence of initial stresses ($\eta = 2.5$, $p = 1$) and in absence of initial stresses ($\eta = 1$, $p = 0$), respectively.

In presence of initial stresses, the amplitude ratio of reflected qP wave attains its maximum value near normal incidence of an incident qT wave. It decreases sharply to its minima near $\theta_0 = 75^\circ$; thereafter, it increases sharply. The variation is shown graphically in Fig. 2 by a solid curve. In absence of initial stresses, the solid curve reduces to a dotted curve, as shown in Fig. 2. The comparison of these two curves shows the effect of initial stresses on the reflected qP wave.

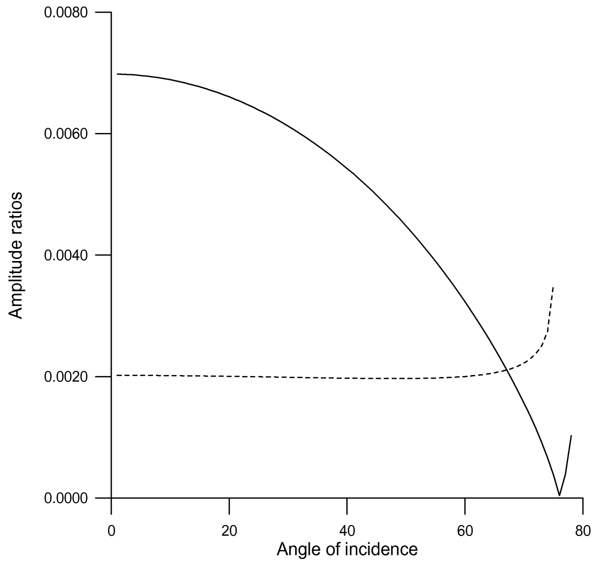

FIG. 2. Variations of amplitude ratios of reflected P waves with the angle of incidence in presence (solid curve) and in absence (dotted curve) of initial stresses.

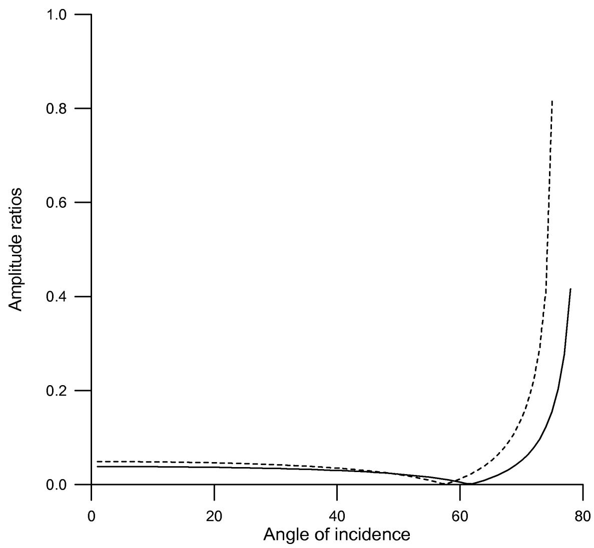

FIG. 3. Variations of amplitude ratios of reflected thermal waves with the angle of incidence in presence (solid curve) and in absence (dotted curve) of initial stresses.

The variations of amplitude ratios for reflected qT waves with the angle of incidence of qT wave, are shown graphically in Fig. 3 by solid and dotted curves in presence and absence of initial stresses, respectively. The amplitude ratios in presence as well as in absence of initial stresses, first decrease slowly to their respective minima, and then increase sharply to their respective maxima.

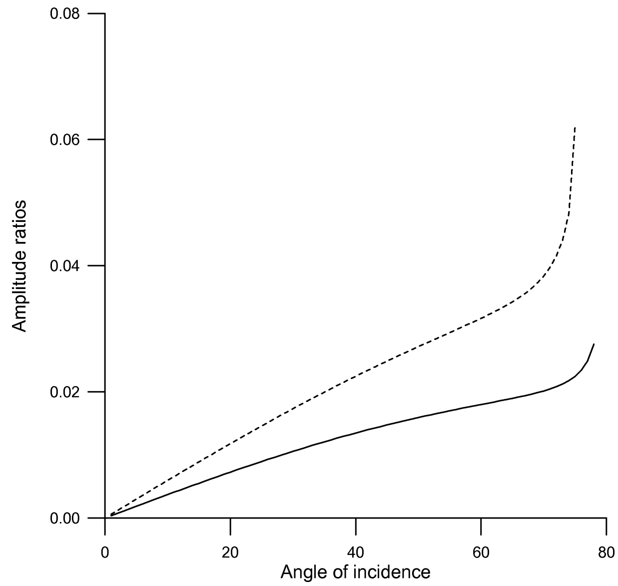

Fig. 4. Variations of amplitude ratios of reflected SV waves with the angle of incidence in presence (solid curve) and in absence (dotted curve) of initial stresses.

The variations of amplitude ratios of reflected SV waves with the angle of incidence of qT waves are shown graphically in Fig. 4 with and without initial stresses. The amplitude ratios of reflected SV wave reach their minima near normal incidence and they increase with the increase in the angle of incidence. The comparison between solid and dotted curves in Fig. 4 shows the effects of initial stresses on the reflected SV wave. The effect also becomes more considerable when the angle of incidence varies from normal to grazing incidence.

The variations of amplitude ratio of refracted qP, qT and SV waves are shown graphically in Figs. 5 to 7 with the angle of incidence of qT wave. These variations are similar to those for reflected qP, qT and SV waves respectively, though different in magnitudes. In these figures, the comparison of solid and dotted curves reveal the effect of initial stresses on the refracted waves. The maximum effect of initial stresses on the reflected qP wave is observed near normal incidence, whereas the effect reaches maximum beyond $\theta_0 = 70°$ for refracted thermal and SV waves.

The critical angle for reflected and refracted waves is observed near $\theta_0 = 78°$ in presence of initial stresses. The critical angle for these waves shifts to $\theta_0 = 75°$, in absence of initial stresses.

The amplitude ratios of reflected and refracted waves are shown graphically in Figs. 8 and 9, respectively, for a range $1 \leq \eta \leq 3.5$ of initial stress parameter, when the initial stress pressure $p = 1$. The solid curves, dotted curves and

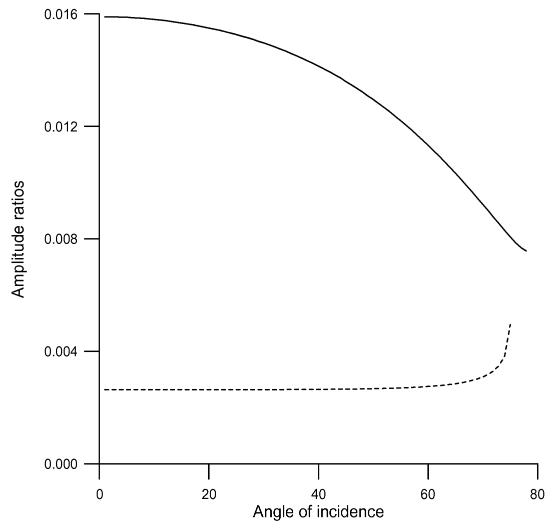

FIG. 5. Variations of amplitude ratios of refracted P waves with the angle of incidence in presence (solid curve) and in absence (dotted curve) of initial stresses.

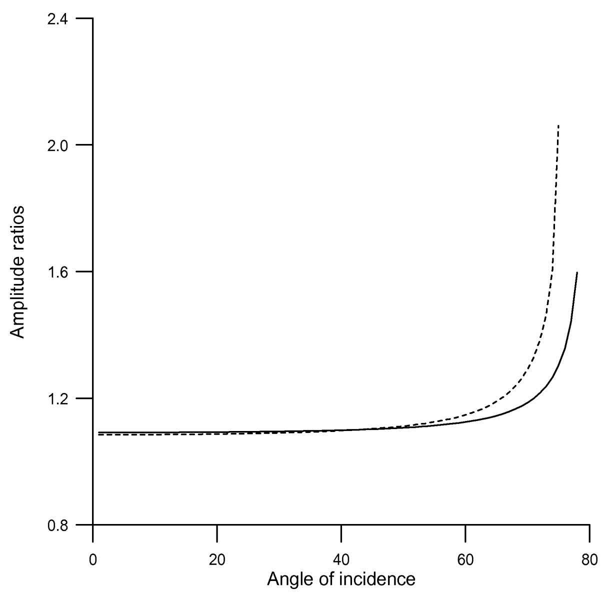

FIG. 6. Variations of amplitude ratios of refracted thermal waves with the angle of incidence in presence (solid curve) and in absence (dotted curve) of initial stresses.

dotted curves with circles in Fig. 8 correspond to reflected qP, reflected qT and reflected SV waves, respectively. Similarly, these curves in Fig. 9 correspond to refracted qP, refracted qT and refracted SV waves, respectively. The amplitude

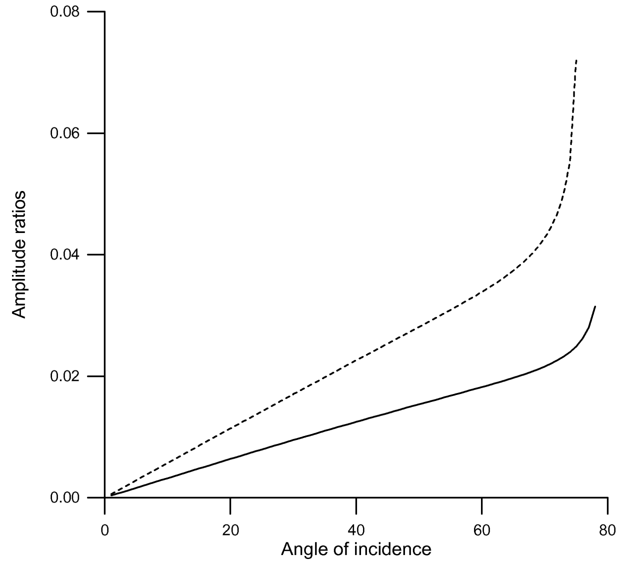

Fig. 7. Variations of amplitude ratios of refracted SV waves with the angle of incidence in presence (solid curve) and in absence (dotted curve) of initial stresses.

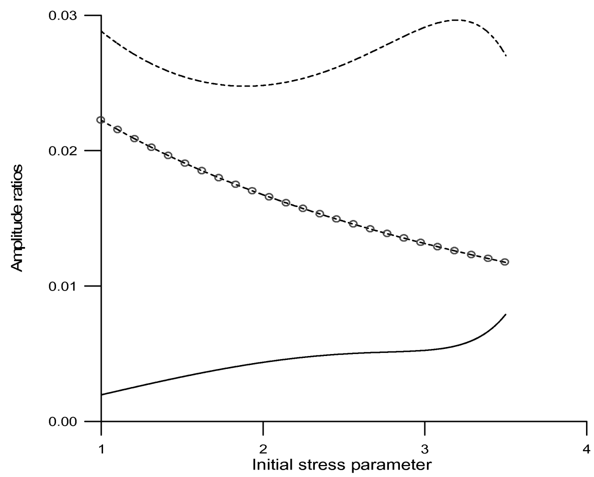

Fig. 8. Variations of amplitude ratios of reflected P wave (solid curve), reflected thermal (dotted curve) and reflected SV wave (dotted curve with circles) with the initial stress parameter η.

ratio of reflected qP wave increase slowly with increase of η. The amplitude ratios of the reflected qT wave oscillate in the range $1 \leq \eta \leq 3.5$, whereas the amplitude ratios of the reflected SV wave decrease slowly in this range.

The amplitude ratios of refracted P and refracted qT wave increase very slowly in the range $1 \leq \eta \leq 3.5$ of the initial stress parameter, whereas the

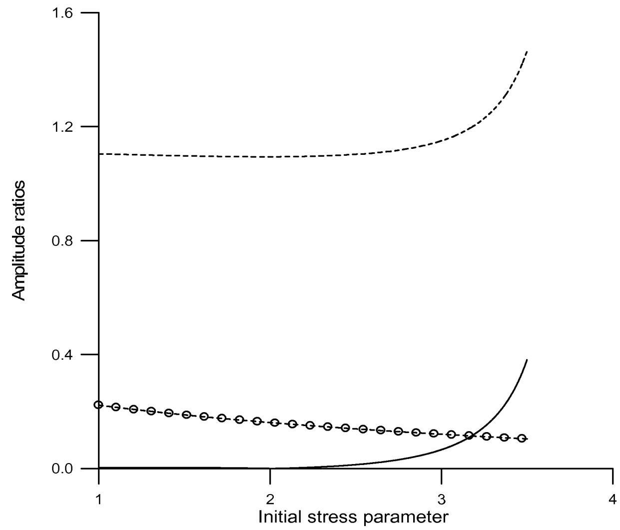

FIG. 9. Variations of amplitude ratios of refracted P wave (solid curve), refracted thermal (dotted curve) and refracted SV wave (dotted curve with circles) with the initial stress parameter η.

amplitude ratios for refracted SV waves decrease slowly for this angle. The dotted curve with circles (refracted SV waves) is shown in Fig. 9 after multiplying its original values by 10.

5. Concluding remarks

The boundary conditions at an interface between two different thermoelastic solid half-spaces with hydrostatic initial stresses in welded contact, are satisfied by relevant potentials for incidence of qT wave to obtain the amplitude ratios of various reflected and refracted waves. These amplitude ratios are computed numerically for a certain range of angle of incidence and initial stress parameter. The amplitude ratios are affected significantly due to the presence of initial stresses. The model discussed in the present paper may provide useful information for experimental seismologists working in the area of wave propagation in solids.

References

1. P. CHADWICK, *Thermoelasticity: the dynamic theory*, [in:] Progress in Solid Mechanics R. HILL & I.N. SNEDDON [Eds.], Vol. I, pp. 263–328. North-Holland, Amsterdam 1960.

2. H.W. LORD, Y. SHULMAN, *A generalized dynamical theory of thermoelasticity*, J. Mech. Phys. Solids, **15**, 299–309, 1967.

3. A.E. GREEN, K.A. LINDSAY, *Thermoelasticity*, J. Elasticity, **2**, 1–7, 1971.

4. D.S. CHANDRASEKHARAIAH, *Thermoelasticity with second sound: a review*, Appl. Mech. Rev., **39**, 355–376, 1986.

5. R.B. HETNARSKI, J. IGNACZAK, *Generalized Thermoelasticity*, J. Thermal Stresses, **22**, 451–476, 1999.

6. H. DERESIEWICZ, *Effect of boundaries on waves in a thermoelastic solid*, J. Mech. Phys. Solids, **8**, 164–172, 1960.

7. A.N. SINHA, S.B. SINHA, *Reflection of thermoelastic waves at a solid half-space with thermal relaxation*, J. Phys. Earth, **22**, 237–244, 1974.

8. S.B. SINHA, K.A. ELSIBAI, *Reflection of thermoelastic waves at a solid half-space with two relaxation times*, J. Thermal Stresses, **19**, 763–777, 1966.

9. A.N. ABD-ALLA, *Relaxation effects on reflection of generalized magneto-thermoelastic waves*, Mech. Res. Comm., **27**, 591–600, 2000.

10. B. SINGH, *Reflection of plane sound wave from a micropolar generalized thermoelastic solid half-space*, J. Sound and Vibration, **235**, 685–696, 2000.

11. J.N. SHARMA, V. KUMAR, D. CHAND, *Reflection of generalized thermoelastic waves from the boundary of a half-space*, J. Thermal Stresses, **26**, 925–942, 2003.

12. S.B. SINHA, K.A. ELSIBAI, *Reflection and refraction of thermoelastic waves at an interface of two semi-infinite media with two relaxation times*, J. Thermal Stresses, **20**, 129–146, 1996.

13. B. SINGH, *Reflection of thermo-viscoelastic waves from free surface in the presence of magnetic field*, Proc. Nat. Acad. Sci., India, **72A II**, 109–120, 2002.

14. A.N. ABD-ALLA, A.A. YAHIA, S.M. ABO-DABAH, *On reflection of the generalized magneto-thermo-viscoelastic plane waves*, Chaos, Solitons Fractals, **16**, 211–231, 2003.

15. B. SINGH, *Reflection of SV waves from the free surface of an elastic solid in generalized thermoelastic diffusion*, J. Sound and Vibration, **291**, 764–778, 2006.

16. Y.Q. SONG, Y.C. ZHANG, H.Y. XU, B.H. LU, *Magneto-thermoelastic wave propagation at the interface between two micropolar viscoelastic media*, Appl. Math. Comp., **176**, 785–802, 2006.

17. B. SINGH, *Wave propagation in a generalized thermoelastic material with voids*, Appl. Math. Comp., **189**, 698–709, 2007.

18. R. KUMAR, M. SINGH, *Reflection/transmission of plane waves at an imperfectly bonded interface of two orthotropic generalized thermoelastic half space*, Mat. Sci. Engg., **472**, 83–96, 2008.

19. M.I.A. OTHMAN, YAQIN SONG, *Reflection of magneto-thermoelastic waves with two relaxation times and temperature dependent elastic module*, Applied Mathematical Modelling, **32**, 483–500, 2008.

20. M.A. BIOT, *Mechanics of incremental deformations*, John Wiley and Sons, Inc., New York 1965.

21. A. CHATTOPADHYAY, S. BOSE, M. CHAKRABORTY, *Reflection of elastic waves under initial stress at a free surface*, J. Acoust. Soc. Am., **72**, 255–263, 1982.

22. R.S. SIDHU, S.J. SINGH, *Comments on "Reflection of elastic waves under initial stress at a free surface*, J. Acoust. Soc. Am., **72**, 255–263, 1982.; J. Acoust. Soc. Am., **74**, 1640–1642, 1983.

23. S. DEY, N. ROY, A. DUTTA, *Reflection and refraction of P-waves under initial stresses at an interface*, Indian J. Pure Appl. Math., **16**, 1051–1071, 1985.

24. M.M. SELIM, *Reflection of plane waves at free surface of an initially stressed dissipative medium*, Proceedings of World Academy of Sciences, Engineering and Technology, Vol. 30, ISSN 13070-6884, 2008.

25. A. MONTANARO, *On singular surface in isotropic linear thermoelasticity with initial stress*, J. Acoust. Soc. Am., **106**, 1586–1588, 1999.

26. B. SINGH, A. KUMAR, J. SINGH, *Reflection of generalized thermoelastic waves from a solid half-space under hydrostatic initial stress*, Applied Mathematics and Computation, **177**, 170–177, 2006.

27. B. SINGH, *Effect of hydrostatic initial stresses on waves in a thermoelastic solid half-space*, Applied Mathematics and Computation, **198**, 494–505, 2008.

28. M.I.A. OTHMAN, Y. SONG, *Reflection of plane waves from an elastic solid half-space under hydrostatic initial stress without energy dissipation*, International Journal Solids and Structures, **44**, 5651–5664, 2007.

29. W.H. WEISKOPF, *Stresses in soils under a foundation*, Journal of Franklin Institute, **239**, 445–450, 1945.

Received April 7, 2009; revised version February 9, 2010.